

# Numerical Solution of Steady Magnetohydrodynamic Boundary Layer Flow Due to Gyrotactic Microorganism for Williamson Nanofluid over Stretched Surface in the Presence of Exponential Internal Heat Generation

M. A. Talha, M. Osman Gani, M. Ferdows

**Abstract**—This paper focuses on the study of two dimensional magnetohydrodynamic (MHD) steady incompressible viscous Williamson nanofluid with exponential internal heat generation containing gyrotactic microorganism over a stretching sheet. The governing equations and auxiliary conditions are reduced to a set of non-linear coupled differential equations with the appropriate boundary conditions using similarity transformation. The transformed equations are solved numerically through spectral relaxation method. The influences of various parameters such as Williamson parameter  $\gamma$ , power constant  $\lambda$ , Prandtl number  $P_r$ , magnetic field parameter  $M$ , Peclet number  $P_e$ , Lewis number  $Le$ , Bioconvection Lewis number  $L_b$ , Brownian motion parameter  $N_b$ , thermophoresis parameter  $N_t$ , and bioconvection constant  $\sigma$  are studied to obtain the momentum, heat, mass and microorganism distributions. Moment, heat, mass and gyrotactic microorganism profiles are explored through graphs and tables. We computed the heat transfer rate, mass flux rate and the density number of the motile microorganism near the surface. Our numerical results are in better agreement in comparison with existing calculations. The Residual error of our obtained solutions is determined in order to see the convergence rate against iteration. Faster convergence is achieved when internal heat generation is absent. The effect of magnetic parameter  $M$  decreases the momentum boundary layer thickness but increases the thermal boundary layer thickness. It is apparent that bioconvection Lewis number and bioconvection parameter has a pronounced effect on microorganism boundary. Increasing brownian motion parameter and Lewis number decreases the thermal boundary layer. Furthermore, magnetic field parameter and thermophoresis parameter has an induced effect on concentration profiles.

**Keywords**—Convection flow, internal heat generation, similarity, spectral method, numerical analysis, Williamson nanofluid.

## I. INTRODUCTION

**D**UE to enormous application in electronic, magnetic, optical and thermal properties, wetting and other engineering applications, nanofluid and fluid-suspension of nanostructures have become very popular nowadays. The idea behind its popularity is very simple. As we know that the common fluids (water, ethylene glycol, engine oil) have low heat transfer abilities as they have the low thermal conductivity, therefore for improving heat transfer capabilities nanofluids

plays a very vital role as they contain metal in it. The introduction of nanofluid has been introduced by Choi [1]. After these work lots of researchers have made useful contribution that involved nanoparticles [2], [3].

The interest on non-Newtonian fluid has increased remarkably due to its diverse application in engineering field. So, in this process, lots of pseudo plastic models [4], [5] are proposed to investigate the pseudo plastic properties. Williamson fluid is one of the most popular pseudo plastic fluids. It has considerable application in biological engineering [6]. Nadeem and Hussain [7] used Homotopy analysis method (HAM) to investigate 2D flow of heat transfer on Williamson nanofluids. Prasannakumara et al. [8] investigate slip flow over a stretching surface comprising porous medium for Williamson nanofluids in presence of thermal radiation.

Nowadays, nanofluids comprising gyrotactic microorganism have attracted many authors to investigate their various effects on fluid flow problem. Microorganisms play a very important role for reducing greenhouse effect. Microorganisms are more effective for absorbing carbon dioxide other than plants. Platt [9] first introduced the word bioconvection which is now a subdivision of biological fluid dynamics. Different bioconvection systems were studied on the basis of the mechanism of directional motion of the different types of microorganisms by several investigators including [10]-[17]. They discussed that microorganism has a grate rule of nanoparticles. Buongiorno [18] proposed a new model based on the mechanism of nanoparticles in the boundary layer phenomena. After analyzing seven slip mechanisms he found that if the turbulent effects are absent then the Brownian diffusion and the thermophoresis parameters play an important role. A. Aziz and W.A. Khan [19] introduced a general method to analysis the free convection flow embedded in a porous medium due to gyrotactic microorganisms. Dinarvand et al. [20] used Buongiorno's model to examine the nanofluid stagnation point flow by considering the different parameters. Dinarvand [21] applied HAM method to discuss the nanofluid flow over a vertical surface. In this work, our objective is to march the concept Williamson nanofluid with gyrotactic microorganism

M.A. Talha and M. Osman Gani are with Department of Mathematics Jahangirnagar University, Savar, Bangladesh.

M. Ferdows is with Research group of Fluid Flow Modeling and Simulation, Department of Applied Mathematics University of Dhaka, Dhaka-1000, Bangladesh (e-mail: ferdows@du.ac.bd).

to study the 2-D steady, incompressible MHD boundary layer flow, heat, and mass transfer of an electrically conducting fluid over a stretching sheet. For the first time, we incorporate heat, mass and microorganism generations in the energy, concentration and microorganism equations. We set  $f_0(\eta) = 1 - e^{-\eta}$ ,  $F(\eta) = e^{-\eta}$ ,  $\theta(\eta) = e^{-\eta}$ ,  $\phi(\eta) = e^{-\eta}$ ,  $\chi(\eta) = e^{-\eta}$  as test function to satisfy the boundary condition for Gauss-Seidel iterative process during the numerical simulation using SRM through the use of MATLAB. In the next section we present the Mathematical model, SRM method, comparison as well as numerical results to predict the problem physical parameters inside the fluid flow phenomena.

## II. MODEL ANALYSIS

Consider a 2-D MHD steady incompressible viscous Williamson nanofluid comprising gyrotactic microorganism over a stretching sheet with internal heat, mass and microorganism generation. The flow velocity  $(u, v)$  acts along the  $X$  and  $y$  axes respectively. The  $X$ -direction is along the sheet surface and  $y$ -direction is normal to it. The transverse magnetic field  $B_0$  is uniform. Induced magnetic field is omitted due to small Reynolds number. The velocity  $U_w(x)$  at the continuous stretching surface are considered to be linear function of  $X$ . Under these conditions, the boundary layer partial differential equations governing the momentum, heat, concentration, and microorganism are written as [20], [21]:

$$\frac{\partial u}{\partial x} + \frac{\partial v}{\partial y} = 0 \quad (1)$$

$$u \frac{\partial u}{\partial x} + v \frac{\partial u}{\partial y} = \nu \frac{\partial^2 u}{\partial y^2} + \sqrt{2} \nu \Gamma \frac{\partial u}{\partial y} \frac{\partial^2 u}{\partial y^2} - \frac{\sigma B_0^2 u}{\rho} \quad (2)$$

$$u \frac{\partial T}{\partial x} + v \frac{\partial T}{\partial y} - \alpha \frac{\partial^2 T}{\partial y^2} - \tau \left( \frac{D_T}{T_\infty} \left( \frac{\partial T}{\partial y} \right) \left( \frac{\partial T}{\partial y} \right) + D_B \frac{\partial T}{\partial y} \frac{\partial C}{\partial y} \right) + q_\theta''' = 0 \quad (3)$$

$$u \frac{\partial C}{\partial x} + v \frac{\partial C}{\partial y} - D_B \left( \frac{\partial^2 C}{\partial y^2} \right) - \frac{D_T}{T_\infty} \left( \frac{\partial^2 T}{\partial y^2} \right) + q_c''' = 0 \quad (4)$$

$$u \frac{\partial n}{\partial x} + v \frac{\partial n}{\partial y} - D_n \left( \frac{\partial^2 n}{\partial y^2} \right) + \frac{dW_c}{C_w - C_\infty} \frac{\partial}{\partial y} \left( n \frac{\partial C}{\partial y} \right) + q_m''' = 0 \quad (5)$$

The boundary conditions are:

$$\text{At } y=0: u=U_w(x)=bx, v=0, T=T_w=T_\infty + Ax^2,$$

$$n=n_w=n_\infty + Ex^2, C=C_w=C_\infty + Bx^2$$

$$\text{As } y \rightarrow \infty : u \rightarrow 0, T \rightarrow T_\infty, C \rightarrow C_\infty, n \rightarrow n_\infty \quad (6)$$

Here  $T$  is the temperature of the fluid,  $T_w$  is the wall temperature and  $T_\infty$  is the free stream temperature,  $D_B$  is Brownian diffusion coefficient,  $D_T$  is thermophoresis

coefficient,  $B_0$  is the magnetic field strength,  $\sigma$  is the electrical conductivity,  $n$  is the density of the motile microorganism,  $C_p$  is the specific heat at constant pressure,  $C_w$  is the concentration at the surface,  $C_\infty$  is the concentration in the free stream,  $D_n$  is the diffusivity of the microorganisms,  $\tau$  is the effective heat capacitance,  $Wc$  is the constant maximum cell swimming speed,  $A, B, b, c, E$  are constants,  $q_\theta'''$  is the internal heat generation,  $q_c'''$  is the internal concentration generation,  $q_m'''$  is the internal microorganism generation,  $\lambda$  is the power exponent parameter. We consider the following similarity variable as in [8], [10]:

$$\eta = \left( \frac{b}{\nu} \right)^{\frac{1}{2}} y, u = bxf'(\eta), v = -\sqrt{b\nu}f(\eta)$$

$$\chi(\eta) = \frac{n - n_\infty}{n_w - n_\infty}, \theta(\eta) = \frac{T - T_\infty}{T_w - T_\infty}, \phi(\eta) = \frac{C - C_\infty}{C_w - C_\infty} \quad (7)$$

The transformed (1)-(5) become:

$$f'''(1 + \gamma f'') + f f'' - f'^2 - M f' = 0 \quad (8)$$

$$\theta'' + \text{Pr}[f + Nb \phi']\theta' - \text{Pr} \lambda f' \theta + \text{Pr} Nt \theta'^2 + e^{-\eta} = 0 \quad (9)$$

$$\phi'' + Le f \phi' - Le \lambda f' \theta + \frac{Nt}{Nb} \theta'' + e^{-\eta} = 0 \quad (10)$$

$$\chi'' + (\text{Pr} Lb f - Pe \phi')\chi' - (Lb \text{Pr} \lambda f' + Pe \phi'')\chi - Pe \sigma \phi'' + e^{-\eta} = 0 \quad (11)$$

The boundary conditions for the surface and in the distant regime are given by:

$$\eta = 0 : f = 0, f' = 1, \theta = 1, \phi = 1, \chi = 1$$

$$\eta \rightarrow \infty : f' \rightarrow 0, \theta \rightarrow 0, \phi \rightarrow 0, \chi \rightarrow 0 \quad (12)$$

The problem physical parameters are: magnetic field parameter,  $M = \left( \frac{\sigma B_0^2}{b\rho} \right)$ ; Williamson Parameter,  $\gamma = \sqrt{\frac{2b^3}{\nu}} \Gamma x$ ;

Prandtl number,  $\text{Pr} = \frac{\nu}{\alpha}$ ; Peclet number,  $Pe = \left( \frac{dwc}{D_n} \right)$ ;

Brownian motion parameter,  $Nb = \left( \frac{(\rho c_p) D_B (C_w - C_\infty)}{\nu T_\infty (\rho c_f)} \right)$ ;

thermophoresis parameter,  $Nt = \left( \frac{(\rho c_p) D_T (T_w - T_\infty)}{\nu T_\infty (\rho c_f)} \right)$ ; Lewis

number,  $Le = \frac{\nu}{D_B}$ ; Bioconvection Lewis number,  $Lb = \frac{\alpha}{D_n}$ ;

bioconvection parameter,  $\sigma = \frac{n_\infty}{n_w - n_\infty}$ ;

The quantities of most interest are the skin friction

coefficient ( $C_f$ ), the local Nusselt number ( $Nu_x$ ), the local Sherwood number ( $Sh_x$ ) and the density number of the motile microorganism ( $Nn_x$ ). These are:

$$C_f = \frac{2\tau_w}{\rho U_w^2}, Sh_x = \frac{xq_m}{k\Delta T}, Nu_x = \frac{xq_w}{D_B\Delta C}, Nn_x = \frac{xq_n}{D_n\Delta n} \quad (13)$$

where  $\tau_w = -\mu(\partial u/\partial y)_{y=0}$  the surface is shear stress,  $q_w = -k(\partial T/\partial y)_{y=0}$  is the surface heat flux,  $q_m = -D_B(\partial C/\partial y)_{y=0}$  is the surface mass flux,  $q_n = -D_n(\partial n/\partial y)_{y=0}$  is the surface motile microorganism flux. Using these (13) yields:

$$C_f \sqrt{Re_x} = (f''(0)) + \frac{\lambda}{2} f''^2, Re_x^{-1/(n+1)} Nu_x = -\theta'(0),$$

$$Re_x^{-1/2} Sh_x = -\phi'(0), Re_x^{-1/(n+1)} Nn_x = -\chi'(0)$$

where,  $Re_x = \frac{b}{\nu} x^2$  is the local Reynolds number.

### III. SPECTRAL RELAXATION METHOD

For numerical investigations we used an efficient numerical technique called Spectral relaxation method for solving our transformed ordinary differential equations. The key concept of this technique is the use of trial function and test functions [22], [23]. For trial function we use Chebychev polynomials and for test function we used the following assumptions:

$$f(\eta) = 1 - e^{-\eta}, F_0(\eta) = e^{-\eta}, \theta(\eta) = e^{-\eta}, \phi(\eta) = e^{-\eta}, \chi(\eta) = e^{-\eta}$$

The discretization procedure is very similar to Gauss-Seidel discretization idea. In the presence of Joule heating and viscous dissipation Motsa and Makukula [24] investigates the steady von Karman flow using SRM method of a Reiner-Rivlin fluid. Over a stretching surface for Maxwell fluid Shateyi [25] used the SRM to solve the MHD flow and heat transfer. Using the similar technique Shateyi and Makinde [26] studied stagnation point flow of an incompressible viscous fluid. In presence of binary chemical reaction and Arrhenius activation energy complex nonlinear system of equations of incompressible flow are solved using SRM technique by Awad et al. [27] over a stretching surface. Now for our model we discretize the transformed (8) to (11) using the following SRM algorithm:

1. Reduced the order  $f(\eta)$  from three to two by taking  $f'(\eta) = F(\eta)$  and defined the transformed equation in forms of  $F(\eta)$ , and the functions  $\theta(\eta)$ ,  $\phi(\eta)$ ,  $\chi(\eta)$  which are in second order need not required to reduce the order.
2. Rewrite the transformed equation involving iteration notation.
3. In equation for  $F(\eta)$  the scheme is developed by considering that only linear terms in  $F(\eta)$  are evaluated in current i.c r+1 iteration level and all the other terms (linear

and non-linear) in  $f(\eta)$ ,  $\theta(\eta)$ ,  $\phi(\eta)$ ,  $\chi(\eta)$  are assumed to be known from previous iteration (noted as r). Non-linear terms in  $F(\eta)$  are evaluated as previous iteration level.

4. In equation for  $\theta(\eta)$ , all the linear term in  $\theta(\eta)$  and all the term in  $f(\eta)$ ,  $F(\eta)$  are calculated in current iteration level (as the update is available for  $f(\eta)$ ,  $F(\eta)$ ) and other terms will use the value of previous iteration.
5. In similar manner the value of  $\phi(\eta)$ ,  $\chi(\eta)$  will be evaluated.

Using the above three steps, (8)-(11) become:

$$f_{r+1}''' (1 + \gamma f_r'') + f_r f_{r+1}'' - f_r'^2 - M f_{r+1}' = 0 \quad (14)$$

$$\theta_{r+1}'' + Pr [f_{r+1} + Nb \phi_r'] \theta_{r+1}' - Pr \lambda f_{r+1}' \theta_{r+1} + Pr Nt \theta_r'^2 + e^{-\eta} = 0 \quad (15)$$

$$\phi_{r+1}'' + Le f_{r+1}' \phi_{r+1}' - Le \lambda f_{r+1}' \phi_{r+1}' + \frac{Nt}{Nb} \theta_{r+1}'' + e^{-\eta} = 0 \quad (16)$$

$$\chi_{r+1}'' + (Pr Lb f_{r+1}' - Pe \phi_{r+1}') \chi_{r+1}' - (Lb Pr \lambda f_{r+1}' + Pe \phi_{r+1}'') \chi_{r+1} - Pe \sigma \phi_{r+1}'' + e^{-\eta} = 0 \quad (17)$$

subject to boundary conditions:  $F_{r+1}(0)=1; F_{r+1}(\infty)=0;$   
 $\theta_{r+1}(0)=1; \theta_{r+1}(\infty)=0; \phi_{r+1}(0)=1; \phi_{r+1}(\infty)=0;$   
 $\chi_{r+1}(0)=1; \chi_{r+1}(\infty)=0.$  Applying the Chebychev spectral collocation method (14)-(17), we obtain:

$$A_1 F_{r+1} = B_1$$

$$A_2 F_{r+1} = B_2$$

$$A_3 \theta_{r+1} = B_3$$

$$A_4 \phi_{r+1} = B_4$$

$$A_5 \chi_{r+1} = B_5$$

where  $A_1 = \text{diag}(1 + \gamma f_r'') D^2 + \text{diag}[f_r] D - M I; B_1 = F_r'^2; A_2 = D; B_2 = F_{r+1};$   
 $A_3 = D^2 + \text{diag}[Pr(f_{r+1} + Nb \phi_r')] D - \text{diag}[Pr \lambda f_{r+1}']; B_3 = -Pr Nt \theta_r'^2 - e^{-\eta};$   
 $A_4 = D^2 + \text{diag}[Le f_{r+1}'] D - \text{diag}[Le \lambda f_{r+1}']; B_4 = -\frac{Nt}{Nb} \theta_{r+1}'' - e^{-\eta};$

$A_5 = D^2 + \text{diag}[Pr Lb f_{r+1}' - Pe \phi_{r+1}'] D - \text{diag}[(Lb Pr \lambda f_{r+1}' + Pe \phi_{r+1}'')];$

$B_5 = \frac{Nt}{Nb} \theta_{r+1}'' - e^{-\eta}.$  I is an identity matrix and  $\text{diag}[]$  is a diagonal

matrix, all size  $(N+1) \times (N+1)$ , where  $N$  is the number of grid points,  $f, F, h, \theta, \phi, \chi$  respectively, when evaluated at the grid points and the subscript r denotes the iteration number. In our present study we take  $N=80$  collocation point. These values gave accurate result for all the quantities of physical interest. Starting from the initial approximation the SRM scheme is repeatedly solve until the following condition is satisfied:

$$\max (F_{r+1} - F_\infty, \theta_{r+1} - \theta_\infty, \phi_{r+1} - \phi_\infty, \chi_{r+1} - \chi_\infty) \leq \epsilon_r$$

where,  $\varepsilon_r$  is a prescribed error tolerance which in this study is taken to be  $10^{-6}$ . To validate the accuracy of our computations we compared the values of  $-\theta'(0)$ , with existing results [8], [10] by setting  $e^{-\eta} = \gamma = \lambda = Nt = Nb = Le = Lb = Pe = M = \sigma = 0$  and varying the value of Pr. The results are seen better agreement as presented in Table I.

TABLE I  
 COMPARISON OF SKIN FRICTION COEFFICIENT  $-\theta'(0)$  WITH PUBLISHED

Pr	Present Study	Wang [28]	Goyal and Bhargava [29]
0.20	0.1691225	0.1691	0.1691
0.70	0.4539241	0.4539	0.4539
2.0	0.91135765	0.9114	0.9113
7.0	1.89540324	1.8954	1.8954
20.0	3.35390413	3.3539	3.3539

#### IV. RESULTS AND DISCUSSION

Equations (8)-(11) are solved numerically using SRM governed by the boundary conditions (12) in order to see the significance of the problem parameters namely Prandtl number (Pr), magnetic field parameter (M), Peclet number (Pe), Lewis number (Le), Bioconvection Lewis number (Lb), Brownian motion parameter (Nb), thermophoresis parameter (Nt) and bioconvection constant ( $\sigma$ ). The computation of our study has performed for various values of these parameters. In SRM technique, we used Gauss-Seidal discretization process and Chebychev collocation process to grid generation for our transformed (8) to (11) and use MATLAB to get our required calculations. The numerical results have been discussed for various values of non-dimensional parameters:

$$M = 0, 0.5, 1 \quad Nt = 0.1, 0.5, 1.2, \quad Nb = 0.1, 0.5, 1.2, \quad Le = 1, 3, 5, \\ Lb = 0.5, 0.6, 0.7, \quad Pe = 0.3, 0.5, 0.7 \quad c = 0, 1, \quad \sigma = 0.2, 0.4, 0.6, \\ Pr = 0.7, 3, 6, 17, \quad \lambda = 0, 1/3, 1, \quad \gamma = 0, 0.25, 0.5, 0.05$$

in the numerical computations. Fig. 1 describes the velocity, temperature, concentration and microorganism profiles in presence or absence of internal generations for different values of Williamson parameter  $\gamma$ . The profiles are plotted against the similarity variable  $\eta$ . For velocity profile no impact is noticed for internal heat generation, but it starts to decrease as Williamson parameter increases. On the other side temperature, concentration and gyrotactic microorganism profiles show significant impact for internal generations when the value of  $\gamma$  increases. We find these profiles increasing with the increase of Williamson parameter. It is evident that within the boundary layer the internal generation takes place with an increase for all three boundaries on energy, mass and microorganism profiles. A similar behavior was observed for without internal generations.

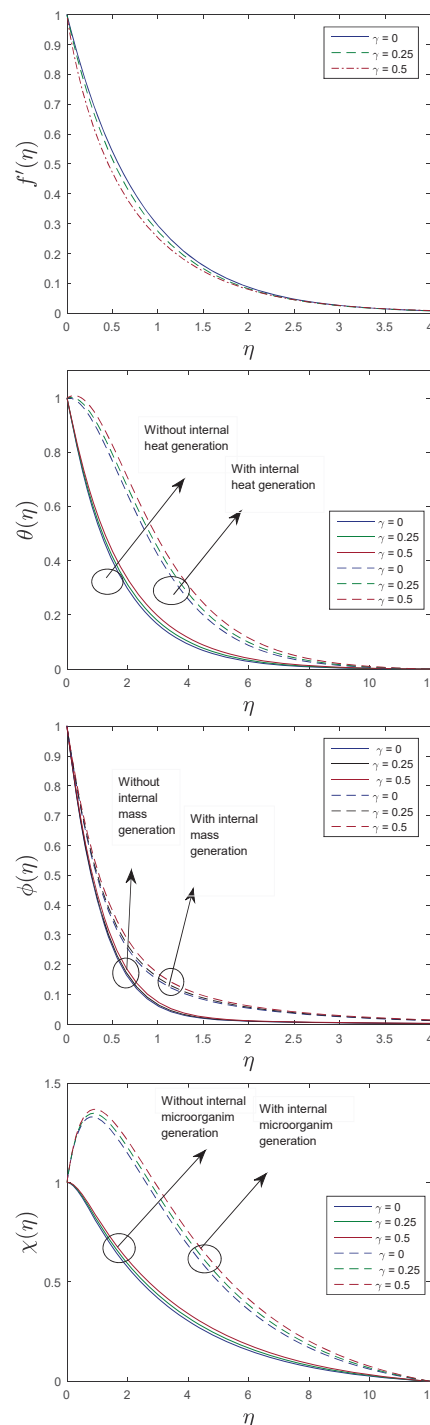


Fig. 1 Profiles of  $f'(\eta)$   $\theta(\eta)$   $\phi(\eta)$   $\chi(\eta)$  for various values of  $\gamma$   
 $M = 0.5, Nb = 0.5, Nt = 0.1, Le = 5, Lb = 0.5, Pe = 0.3, \sigma = 0.2, Pr = 0.7, c = 0, 1, \lambda = 1/3$

Fig. 2 illustrates the effect of M on the velocity, temperature, concentration and gyrotactic microorganism profiles. It is clear that increase of magnetic field strength leads to decrease the velocity profile and the fact is that the Lorentz force arising in this case reduces the flow in the boundary layer. Also, the temperature, concentration and gyrotactic microorganism thin

layer increases at different values of the magnetic parameter. We also observe a large effect on the velocity but a relatively small influence on the other profiles and this is due to the fact that the magnetic forces are strongly related with velocity boundary. It is also clear that an inverse in M leads to increase in the temperature, concentration, and microorganism of the fluid.

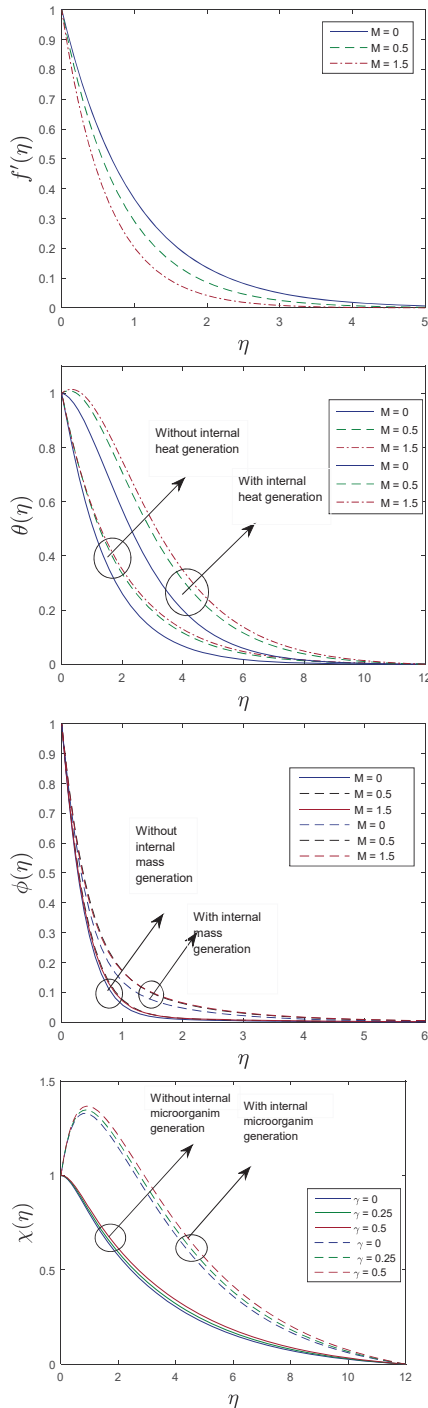


Fig. 2 Profiles of  $f'(\eta)$   $\theta(\eta)$   $\phi(\eta)$   $\chi(\eta)$  for various values of M  $\gamma = 0.05$ ,  $Nb = 0.5$ ,  $Nt = 0.1$ ,  $Le = 5$ ,  $Lb = 0.5$ ,  $Pe = 0.3$ ,  $\sigma = 0.2$   $Pr = 0.7$ ,  $c = 0,1$ ,  $\lambda = 1/3$

Fig. 3 describes the velocity, temperature, concentration and gyrotactic microorganism profiles at various values of power exponent parameter  $\lambda$ . The value of  $\lambda = 0$  correspond to uniform surface temperature/concentration/microorganism, whereas  $\lambda = 1/3$  correspond to uniform surface flux and  $\lambda = 1$  corresponds to uniform wall temperature/concentration/microorganism. We observe that temperature, concentration and gyrotactic microorganism profile decreases as the power exponent parameter increases, whereas this effect is seen very significant for temperature and microorganism boundary with internal heat and microorganism generations respectively than that of concentrations boundary layer.

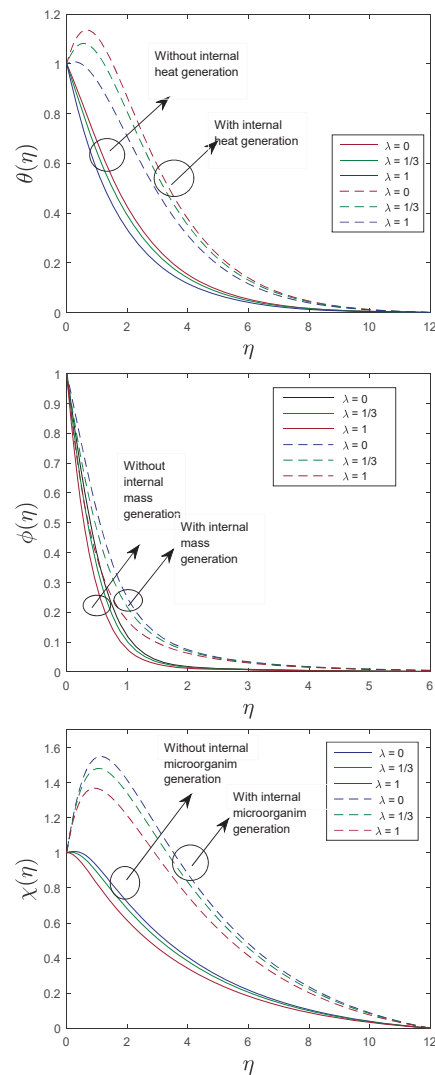


Fig. 3 Profiles of  $f'(\eta)$   $\theta(\eta)$   $\phi(\eta)$   $\chi(\eta)$  for various values of  $\lambda$   $\gamma = 0.05$ ,  $Nb = 0.5$ ,  $Nt = 0.1$ ,  $Le = 5$ ,  $Lb = 0.5$ ,  $Pe = 0.3$ ,  $\sigma = 0.2$   $Pr = 0.7$ ,  $c = 0,1$ ,  $M = 0.5$

Fig. 4 describes the temperature, concentration and gyrotactic microorganism profiles for diverse values of Prandtl number. It is found that for all the cases i.e temperature, concentration and volume fraction of gyrotactic microorganism

boundary layer decreases with the increase of the Prandtl number for all three types of internal generation.

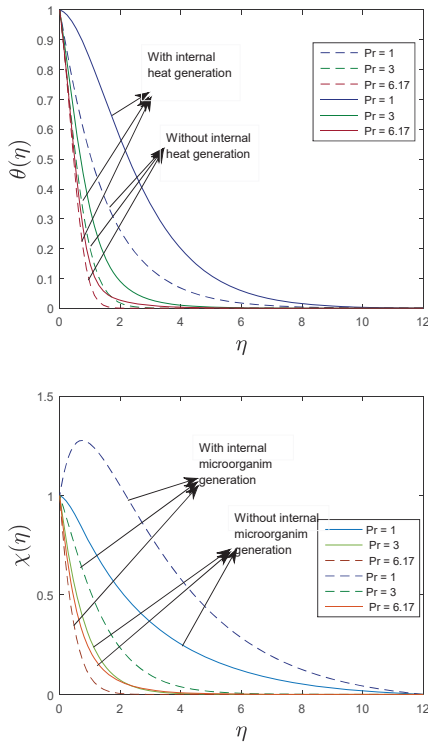


Fig. 4 Profiles of  $f'(\eta)$   $\theta(\eta)$   $\phi(\eta)$   $\chi(\eta)$  for various values of  $Pr$   $\gamma = 0.05$ ,  $Nb = 0.5$ ,  $Nt = 0.1$ ,  $Le = 5$ ,  $Lb = 0.5$ ,  $Pe = 0.3$ ,  $\sigma = 0.2$ ,  $\lambda = 1/3$ ,  $c = 0,1$ ,  $M = 0.5$

Fig. 5 illustrates the temperature and concentration profile for different values of thermophoresis parameter  $Nt$ . The value of  $Nt$  can be positive or negative. Positive values correspond to hot surface and negative values corresponds to cool surface. The nanofluid velocity and motile microorganism profile are not affected with  $Nt$ . As the value of  $Nt$  increases the temperature and concentration profile increases.

Fig. 6 describes the temperature and concentration profiles for different values of Brownian motion parameter  $Nb$ . The nanofluid velocity and motile microorganism profile is not affected with  $Nb$ . From Fig. 6, it is clear that as the raising value of  $Nb$  leads to increase the temperature boundary layer but decreases the concentration boundary thickness.

Fig. 7 describes the concentration and the gyrotactic microorganism profile for different values of Lewis number  $Le$ . The surface shear stress and Nusselt number are not influenced by any change of  $Le$ , so the nanofluid velocity and temperature are not affected too. From the figure, we can see that increase of  $Le$  results in decreasing concentration profile whereas  $Le$  leads to increase in the microorganism boundary layers.

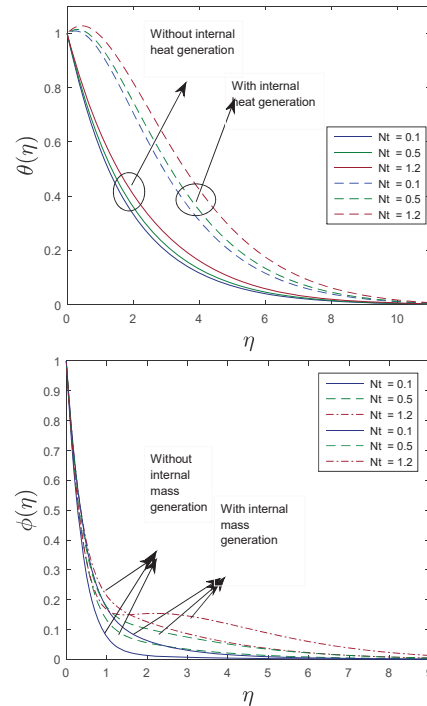


Fig. 5 Profiles of  $\theta(\eta)$  and  $\phi(\eta)$  for different values of  $Nt$   $\gamma = 0.05$ ,  $Nb = 0.5$ ,  $Le = 5$ ,  $Lb = 0.5$ ,  $Pe = 0.3$ ,  $\sigma = 0.2$ ,  $\lambda = 1/3$ ,  $c = 0,1$ ,  $M = 0.5$ ,  $Pr = 0.71$

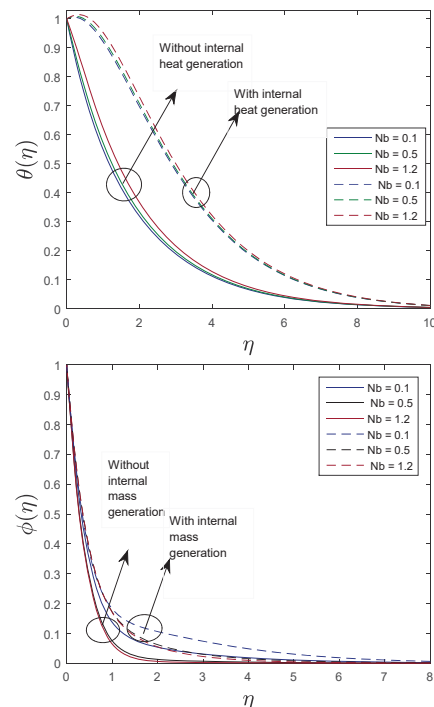


Fig. 6 Profiles of  $\theta(\eta)$  and  $\phi(\eta)$  for various values of  $Nb$   $\gamma = 0.05$ ,  $Nt = 0.1$ ,  $Le = 5$ ,  $Lb = 0.5$ ,  $Pe = 0.3$ ,  $\sigma = 0.2$ ,  $\lambda = 1/3$ ,  $c = 0,1$ ,  $M = 0.5$ ,  $Pr = 0.71$

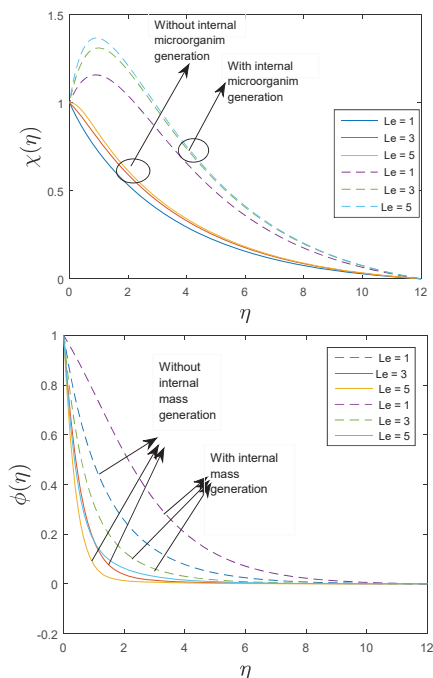


Fig. 7 Profiles of  $\phi(\eta)$  and  $\chi(\eta)$  for different values of  $Le$   
 $\gamma = 0.05, Nt = 0.1, Nb = 0.5, Lb = 0.5, Pe = 0.3, \sigma = 0.2,$   
 $\lambda = 1/3, c = 0,1, M = 0.5, Pr = 0.71$

From Fig. 8 we observed reduction in the boundary layer thickness of the motile microorganism for increasing values of the bioconvection Lewis number  $Lb$  and bioconvection parameter  $\sigma$  but for increasing Peclet number  $Pe$  the boundary layer thickness of microorganism induces.

Fig. 9 shows the residual error of (8)-(11) in presence or absence of internal generations against iterations for different values power exponent parameter. The residual error of  $\theta(\eta), \phi(\eta), \chi(\eta)$  take linear shapes and are iteration dependent. The increasing value of  $\lambda$  leads to decrease the residual error and accelerate the convergence. Faster convergence is achieved when internal heat generation is absent.

Fig. 10 illustrates skin friction, Nusselt number, Sherwood number and the density number of the motile microorganism respectively for different values of Williamson parameter. The value is plotted against the power law parameter  $\lambda$ . As the value of magnetic parameter increases shear stress decreases. On the other hand, temperature, concentration and microorganism gradient profiles are increasing function of the Williamson parameter.

Fig. 11 illustrates the density number of the motile microorganism for different values of Bioconvection Lewis number and Bioconvection parameter. The microorganism gradient profiles are increasing function of  $Pe$  and  $Lb$ .

#### V.CONCLUSION

In the present study, we consider two dimensional MHD steady incompressible flow, heat and mass transfer of

Williamson nanofluid comprising gyrotactic microorganism over stretching sheet in presence of internal heat generation. The effect of magnetic field, Brownian diffusion and Thermophoresis are taking into account.

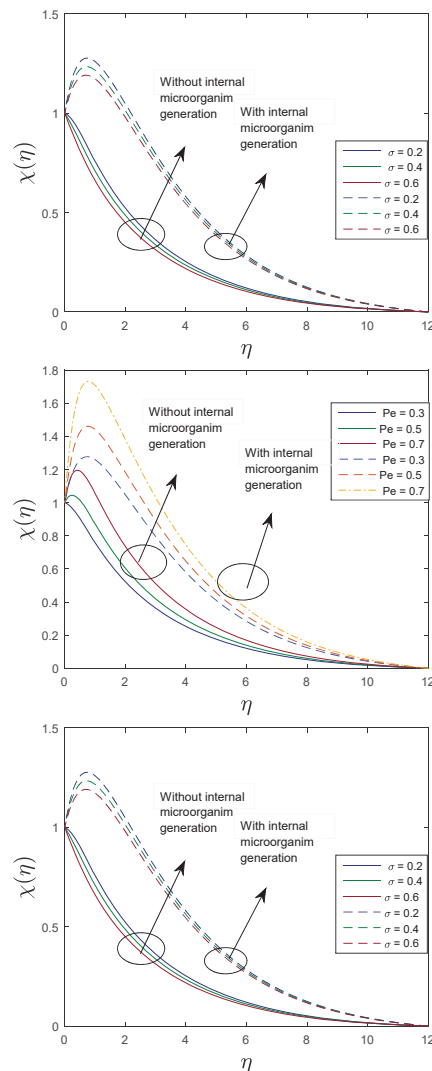


Fig. 8  $\chi(\eta)$  profiles, for different values of  $\sigma, Pe, Lb$   
 $\gamma = 0.05, Nt = 0.1, Nb = 0.5, Lb = 0.5, 0.6, 0.7, Pe = 0.3, 0.5, 0.7,$   
 $\sigma = 0.2, 0.4, 0.6, \lambda = 1/3, c = 0,1, M = 0.5, Pr = 0.71$

By using non-dimensional form of similarity transformation for velocity, temperature, concentration and microorganism, the basic PDE's governing the flow and heat transfer were transformed into a set of ordinary differential equations and have been solved numerically using SRM method.

Effects of Williamson parameter  $\gamma$ , Prandtl number  $Pr$ , magnetic field parameter  $M$ , Peclet number  $Pe$ , Lewis number  $Le$ , Bioconvection Lewis number  $Lb$ , Brownian motion parameter  $Nb$ , thermophoresis parameter  $Nt$  and bioconvection constant  $\sigma$ , power parameter  $\lambda$ , residual error, heat transfer rate, mass flux rate and the density number of the motile microorganism have been examined.

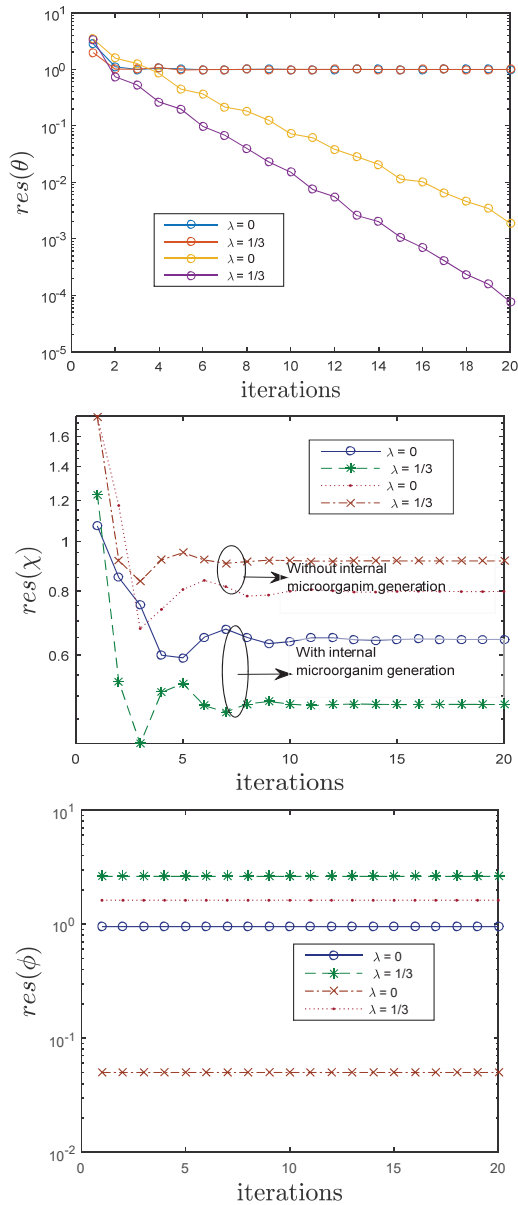


Fig. 9 Residual error of  $\theta(\eta)$   $\phi(\eta)$   $\chi(\eta)$  against iterations for different values of  $\lambda$   
 $\gamma = 0.05, Nt = 0.1, Nb = 0.5, Lb = 0.5, Pe = 0.3, \sigma = 0.2, \lambda = 1/3, M = 0.5, Pr = 0.71$

We found that:

- $M, Nt, Nb, Pr$  enhance the temperature field  $\theta$  for both stretching and shirking sheet.
- The flow is more significant with internal generations and this induce the mechanical strength in the fluid boundary layer.
- $M$  is a decreasing function of  $f'(\eta)$ .
- The density of the motile microorganism  $\chi$  is a decreasing function of  $Pe, \sigma, Lb$
- The concentration decreases with the increase of  $Nb, Pr, Le$  while the profiles are found to be more

pronounced with the increase of  $Nt, M$ .

- The residual error of,  $\theta(\eta), \chi(\eta), \phi(\eta)$  are iteration dependent.
- Convergence is faster when internal generations are absent in all flows.

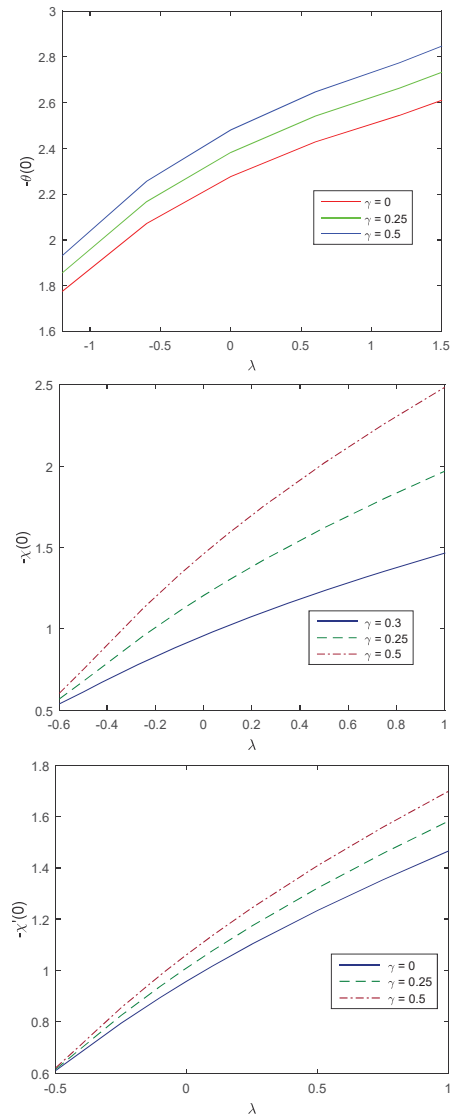
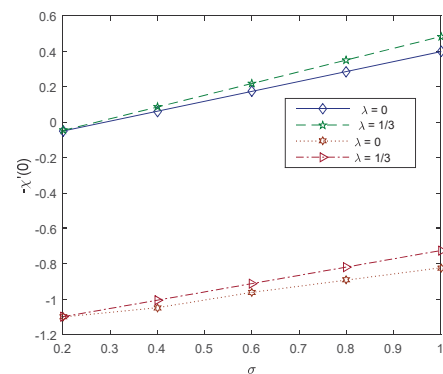


Fig. 10 Nusselt number and Sherwood number for different values of  $Nt$  and  $Nb$





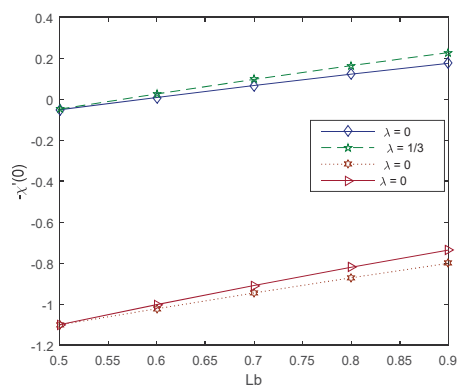


Fig. 11 Density number of the motile microorganism for different values of  $Lb, \sigma$

#### REFERENCES

[1] Choi, S. U. S., Zhang, Z. G., Yu, W., Lockwood, F. E., & Grulke, E. A. "Anomalous thermal conductivity enhancement in nanotube suspensions," *Applied physics letters*, 79(14), 2252-2254, 2001

[2] Venkateswarlu, B., Narayana, P. S. "Chemical reaction and radiation absorption effects on the flow and heat transfer of a nanofluid in a rotating system," *Applied Nanoscience*, 5(3), 351-360, 2015

[3] Reddy, M. G. "Influence of magnetohydrodynamic and thermal radiation boundary layer flow of a nanofluid past a stretching sheet," *Journal of Scientific Research*, 6(2), 257-272, 2014

[4] Sorbie, K. S., Clifford, P. J., Jones, E. R. W. "The rheology of pseudoplastic fluids in porous media using network modeling," *Journal of Colloid and Interface Science*, 130(2), 508-534, 1989

[5] Pakzad, L., Ein-Mozaffari, F., Chan, P. "Using electrical resistance tomography and computational fluid dynamics modeling to study the formation of cavern in the mixing of pseudoplastic fluids possessing yield stress," *Chemical Engineering Science*, 63(9), 2508-2522, 2008

[6] Kothandapani, M., Prakash, J. "Effects of thermal radiation parameter and magnetic field on the peristaltic motion of Williamson nanofluids in a tapered asymmetric channel," *International Journal of Heat and Mass Transfer*, 81, 234-245, 2015

[7] Nadeem, S., Hussain, S. T. "Flow and heat transfer analysis of Williamson nanofluid," *Applied Nanoscience*, 4(8), 1005-1012, 2014

[8] Prasannakumara, B. C., Gireesha, B. J., Gorla, R. S., & Krishnamurthy, M. R. "Effects of chemical reaction and nonlinear thermal radiation on Williamson nanofluid slip flow over a stretching sheet embedded in a porous medium," *Journal of Aerospace Engineering*, 29(5), 04016019, 2016

[9] Platt, J. R. "Bioconvection Patterns" in Cultures of Free-Swimming Organisms," *Science*, 133(3466), 1766-1767, 1961

[10] Kuznetsov, A. V. "Bio-thermal convection induced by two different species of microorganisms," *International Communications in Heat and Mass Transfer*, 38(5), 548-553, 2011

[11] Kuznetsov, A. V. "The onset of thermo-bioconvection in a shallow fluid saturated porous layer heated from below in a suspension of oxytactic microorganisms," *European Journal of Mechanics-B/Fluids*, 25(2), 223-233, 2006

[12] Nield, D. A., Kuznetsov, A. V. "The onset of bio-thermal convection in a suspension of gyrotactic microorganisms in a fluid layer: oscillatory convection," *International journal of thermal sciences*, 45(10), 990-997, 2006

[13] Avramenko, A. A., Kuznetsov, A. V. "Stability of a suspension of gyrotactic microorganisms in superimposed fluid and porous layers," *International communications in heat and mass transfer*, 31(8), 1057-1066, 2004

[14] Alloui, Z., Nguyen, T. H., Bilgen, E. "Numerical investigation of thermo-bioconvection in a suspension of gravitactic microorganisms," *International journal of heat and mass transfer*, 50(7), 1435-1441, 2007

[15] Mahdy, A. "Gyrotactic Microorganisms Mixed Convection Nanofluid Flow along an Isothermal Vertical Wedge in Porous Media," *World Academy of Science, Engineering and Technology, International Journal of Mechanical, Aerospace, Industrial, Mechatronic and Manufacturing*

*Engineering*, 11(4), 829-839, 2017

[16] Tham, L., Nazar, R., & Pop, I. "Steady mixed convection flow on a horizontal circular cylinder embedded in a porous medium filled by a nanofluid containing gyrotactic micro-organisms," *Journal of Heat Transfer*, 135(10), 102601, 2013

[17] Kuznetsov, A. V. "The onset of nanofluid bioconvection in a suspension containing both nanoparticles and gyrotactic microorganisms" *International Communications in Heat and Mass Transfer*, 37(10), 1421-1425, 2010

[18] Buongiorno, J. "Convective transport in nanofluids," *Journal of Heat Transfer*, 128(3), 240-250, 2006

[19] Aziz, A., Khan, W. A., Pop, I. "Free convection boundary layer flow past a horizontal flat plate embedded in porous medium filled by nanofluid containing gyrotactic microorganisms," *International Journal of Thermal Sciences*, 56, 48-57, 2012

[20] Kho, Y. B., Hussanan, A., Mohamed, M. K. A., Sarif, N. M., Ismail, Z., & Salleh, M. Z. "Thermal radiation effect on MHD Flow and heat transfer analysis of Williamson nanofluid past over a stretching sheet with constant wall temperature," In *Journal of Physics: Conference Series* (Vol. 890, No. 1, p. 012034). IOP Publishing, 2017

[21] Babu, M. J., Sandeep, N. "Effect of nonlinear thermal radiation on non-aligned bio-convective stagnation point flow of a magnetic-nanofluid over a stretching sheet" *Alexandria Engineering Journal*, 55(3), 1931-1939, 2016

[22] Haroun, N. A., Sibanda, P., Mondal, S., Motsa, S. S. "On unsteady MHD mixed convection in a nanofluid due to a stretching/shrinking surface with suction/injection using the spectral relaxation method," *Boundary value problems*, 2015(1), 24, 2015

[23] C. Canuto, M.Y. Hussaini, A. Quarteroni and T.A. Zang, *Spectral Methods in Fluid Dynamics*, Springer-Verlag, Berlin., 1988

[24] Motsa, S. S., Makukula, Z. G. On spectral relaxation method approach for steady von Kármán flow of a Reiner-Rivlin fluid with Joule heating, viscous dissipation and suction/injection. *Central European Journal of Physics*, 11(3), 363-374, 2013

[25] S. Shateyi, A new numerical approach to MHD flow of a Maxwell fluid past a vertical stretching sheet in the presence of thermophoresis and chemical reaction, *Boundary Value Problems*, 196 (2013) .

[26] Shateyi, S., & Makinde, O. D. "Hydromagnetic stagnation-point flow towards a radially stretching convectively heated disk" *Mathematical Problems in Engineering*, 2013.

[27] Awad, F. G., Motsa, S., Khumalo, M. "Heat and mass transfer in unsteady rotating fluid flow with binary chemical reaction and activation energy" *PLoS one*, 9(9), e107622, 2014

[28] Wang, C. Y. "Free convection on a vertical stretching surface," *Journal of Applied Mathematics and Mechanics/Zeitschrift für Angewandte Mathematik und Mechanik*, 69(11), 418-420, 1989

[29] Gorla, R. S. R., Sidawi, I. "Free convection on a vertical stretching surface with suction and blowing," *Applied Scientific Research*, 52(3), 247-257, 1994